Stark broadening data for ultraviolet lines of Ni v

Rafik Hamdi, Sylvie Sahal-Bréchot, Milan S Dimitrijević, Haykel Elabidi

Monthly Notices of the ROYAL ASTRONOMICAL SOCIETY

MNRAS **528,** 6347–6353 (2024) https://doi.org/10.1093/mnras/stae391
Advance Access publication 2024 February 7

Stark broadening data for ultraviolet lines of Ni V

Rafik Hamdi [1]★ Sylvie Sahal-Bréchot [2] Milan S. Dimitrijević [2,3]★ and Haykel Elabidi [4]★

[1]*Departement of Physics, Faculty of Sciences of Bizerte (FSB), 7021 Zarzouna, University of Carthage, Tunis, Tunisia*
[2]*Observatoire de Paris, PSL University, Sorbonne Universite´, CNRS, LERMA, 92190 Meudon, France*
[3]*Astronomical Observatory, Volgina 7, Belgrade 11060, Serbia*
[4]*Physics Department, College of Sciences, Umm Al-Qura University, Makkah Almukarramah 24382, Saudi Arabia*

Accepted 2024 January 30. Received 2024 January 10; in original form 2023 May 27

ABSTRACT

We provide in this work Stark broadening data (widths and shifts) for 120 ultraviolet spectral lines of Ni V ion. Our calculations are performed using the semiclassical perturbation method. For energy levels and oscillator strength calculations, we use the multiconfiguration Hatree–Fock approach. Stark shifts and widths are calculated for collisions with electrons and with the positive ions: H^+, He^+, and He^{++}, allowing us to take into account the important perturbers in stellar atmospheres. We compare our Stark widths with estimations obtained using the Cowley formula. Our electron impact Stark widths are also fitted with temperature using a logarithmic formula. Finally, our obtained Stark widths are used to investigate the influence of Stark broadening in the atmospheric conditions of hot DA white dwarfs. Despite the importance of ultraviolet lines of Ni V ion for modelling white dwarf atmospheres and also for investigations of variation of fundamental constants with gravitational potential, we did not find Stark broadening data previously calculated or measured for Ni V ion. The objective of this work is to give the missed data.

Key words: atomic data – atomic processes – line: profiles – stars: atmospheres – stars: white dwarfs.

1 INTRODUCTION

Stark broadening by collisions with electrons and charged particles plays an important role in various fields of physics and astrophysics. Particularly in plasma diagnostic, fusion plasma research, and laser development research. In astrophysics, Stark broadening data (widths and shifts) are especially needed for modelling and investigating high-surface gravity star atmospheres. Stark widths and shifts may also be useful for the study of stellar interiors and radiative transfer. With the development of instruments of observation, such as the Far Ultraviolet Spectroscopy Explorer (FUSE) and the Space Telescope Imaging Spectrograph (STIS), high-resolution spectra are obtained. Atomic and collisional data are an essential ingredient for a better investigation of such spectra (e.g. Rauch et al. 2020). The influence of Stark broadening mechanism in the atmospheres of A and B type stars, white dwarfs, and subdwarfs has been investigated in various papers (Hamdi et al. 2017; Majlinger, Simić & Dimitrijević 2017; Majlinger, Dimitrijević & Srećković 2020; Elabidi 2021; Sahal-Bréchot & Elabidi 2021). At very high temperatures and electron densities, Stark broadening data may play an important role in the modelization of neutron stars (Dimitrijević et al. 2023).

During the last few years, many papers have been devoted to the study of a possible variation of fundamental constants in strong gravitational fields (e.g. Berengut et al. 2013; Hu et al. 2021; Le 2021). White dwarfs provide a perfect environment for studying such variations. In fact, the gravitational potentials of white dwarfs are around five orders of magnitude larger than on Earth. Ultraviolet lines of Fe V and Ni V are of great importance for such research (Berengut et al. 2013). Using ultraviolet lines of Fe V observed in STIS spectrum of the white dwarf G191-B2B, Hu et al. (2021) investigated the variation of the fine structure constant at the surface of the considered star. They found a possible slight variation of this constant. They also suggest the use of Fe IV and Ni V spectral lines for a better investigation of the studied phenomenon. In Le (2021), ultraviolet lines of Ni V observed in the spectrum of white dwarf G191-B2B have been used to study the variation of the gravitational constant (G) in a strong gravitational field. This variation appears as shifts in the observed wavelengths of Ni V spectral lines. For this reason, Stark widths and shifts of UV lines of Ni V ion may be useful for such investigations. In our previous works (Hamdi et al. 2021, 2022), we have calculated Stark broadening data for Fe V ultraviolet spectral lines.

In the present paper, we provide Stark shifts and widths for 120 UV lines of Ni V ion belonging to the transition array 4s–4p. Our calculations of Stark widths and shifts have been performed using semiclassical perturbation approach (SCP) (Sahal-Bréchot 1969a, b) under the physical conditions of white dwarfs. Energy levels and oscillator strengths needed for SCP calculations have been calculated using the Hartree–Fock method with relativistic corrections by employing the Cowan code (Cowan 1981). Our Stark widths and shifts are given for collisions with electrons and also with the following positive ions: H^+, He^+, and He^{++}. The validity of the approximations taken into account has been discussed. We compared our electron impact Stark width with the estimates obtained with Cowley's formula (Cowley 1971). The importance of broadening by

★ E-mail: rfhamdi@uqu.edu.sa (RH); mdimitrijevic@aob.rs (MSD); haelabidi@uqu.edu.sa (HE)

collisions with electrons under the physical conditions of hot DA white dwarfs has been also studied.

Stark broadening parameters obtained by combining the SCP approach and Cowan code (Cowan 1981) for atomic data have been compared to experiments for many ions (Hamdi et al. 2013, 2014, 2018, 2019). Energy levels and oscillator strengths needed for SCP calculations can also be taken from other sources. Recently, Mahmoudi et al. (2023) used a set of atomic data taken from NIST data base to calculate SCP Stark broadening data for S II ion and compare them with the results obtained using the modified semi-empirical approach (Dimitrijević & Konjević 1980) and also with experimental results. In Aloui et al. (2018), Stark widths for Ar VII obtained using SCP approach and quantum mechanical method (Elabidi, Ben Nessib & Sahal-Bréchot 2004) have been compared. The needed atomic data have been calculated using SUPERSTRUCTURE code (Eissner, Jones & Nussbaumer 1974).

2 THE METHOD

Our computational procedure is similar to that previously described in Hamdi et al. (2021, 2022). We give here a brief description of the formalism and the main approximations taken into account. Stark widths and shifts presented in this paper are performed using the semiclassical perturbation approach (SCP; Sahal-Bréchot 1969a, b). The main data needed for SCP calculation are energy levels and oscillator strengths. Compared to other methods, such as the semi-empirical formula (Dimitrijević & Konjević 1980), the SCP approach requires a relatively large set of atomic data. In the case of a lack of atomic data, our SCP method cannot be applied. In this work, the needed set of atomic data is constructed using Cowan code (Cowan 1981), which is based on the Hartree–Fock approach with relativistic corrections (HFR). The use of the atomic data calculated through Cowan code allows us to calculate Stark widths and shifts for a large number of transitions because the time needed for the calculation is reduced compared to the use of external atomic data like those taken from NIST data base (or other data bases). For some ions, the set of oscillator strengths compiled in the NIST data base is not complete enough to perform SCP calculations of Stark widths and shifts. In Hamdi et al. (2021), we have compared Stark broadening widths and shifts calculated using HFR atomic data and atomic data taken from NIST data base. It was found that the deviation does not exceed the precision limit of the SCP method. The use of a mixture of oscillator strengths obtained with different methods leads to a worse agreement with experimental results as shown in Dimitrijević & Sahal-Bréchot (1994).

The atomic model used for HFR calculations of atomic data includes the following set of configurations: $3d^6$, $3d^54s$, $3d^54d$, $3d^55s$, $3d^55d$, $3d^56s$, $3d^56d$ (even parity), and $3d^54p$, $3d^55p$, $3d^56p$ (odd parity). In our calculation of energy levels and oscillator strengths, we use the *ab initio* procedure since only the three first programs of Cowan are used: RCN, RCN2, and RCG. Single configuration wave functions are calculated using RCN program. RCN2 program calculates dipole integrals, the multiple configurations radial integrals, and Bessel integrals. RCG program is used to calculate the angular factors and radiative data. The fourth program of Cowan code sequence (RCE) used for fitting with experimental energies is not used here.

A description of SCP approach with innovations is given in (Sahal-Bréchot 1969a, b, 1974; Dimitrijević, Sahal-Bréchot & Bommier 1991; Dimitrijević & Sahal-Bréchot 1996; Sahal-Bréchot, Dimitrijević & Nessib 2014; Sahal-Bréchot 2021).

The impact approximation means that the mean duration τ of an interaction is much smaller than the mean interval between two collisions ΔT. This can be written as

$$\tau \ll \Delta T,$$

where $\tau \approx \frac{\rho_{\rm typ}}{v_{\rm typ}}$, $\rho_{\rm typ}$ is a mean typical impact parameter and $v_{\rm typ}$ is a mean typical relative velocity. The mean interval between two collisions ΔT is of the order of the inverse of the collisional line width, which can roughly be written as equal to $N v_{\rm typ} \rho_{\rm typ}^2$, where N is the perturber density. Thus, we can write the condition of validity of the impact approximation as $NV \ll 1$, where $V = \rho_{\rm typ}^3$ is the collision volume.

The SCP method applies when the neighbouring levels do not overlap and the line is considered isolated. It is not the case for lines arising from high levels or at high densities when the electron impact width can be comparable to the separation between the initial or final level and the perturbing energy levels. We give for each studied spectral line, the parameter C defined in Dimitrijević & Sahal-Bréchot (1984). When it is divided by the corresponding Stark width, the parameter C gives an estimation for the maximal perturber density for which the line may be considered isolated.

For collisions with electrons, the contribution of Feshbach resonances is taken into account in SCP calculations (Fleurier, Sahal-Bréchot & Chapelle 1977). Sahal-Bréchot (2021) revisits the determination of semiclassical limit of Feshbach resonances using Gailitis approximation. It was found that their order of magnitude is important at low temperatures but not for all cases.

3 COMPARISON WITH APPROXIMATE FORMULA AND FITTING WITH TEMPERATURE

In order to give an idea about the accuracy of our atomic structure results used as input data for Stark broadening calculations, we compare in Table 1 our calculated wavelengths, weighted oscillator strengths (gf), and transition probabilities (A_{ji}) with the results found in Kurucz data base (2023). As we can see in Table 1, our wavelengths agree with Kurucz ones within 1 per cent on average. The agreement between our weighted oscillator strengths and the values taken from Kurucz data base is within 14 per cent on average. As we can see from Table 1, our atomic data are sufficiently accurate to be adopted for SCP calculations of Stark broadening parameters.

In Table 2, we compare our electron impact Stark widths with the approximate values obtained using Cowley formula (Cowley 1971) for the electron density 10^{17} cm^{-3} and temperature 10 kK. All spectral lines shown in Table 2 are chosen by Preval et al. (2013, 2019) to determine the photospheric abundance of nickel in the hot DA white dwarf G191-B2B and also in metal-polluted white dwarfs. According to Majlinger, Simić & Dimitrijević (2017), taking into account the contribution of the lower level, Cowley's approximate widths are obtained in Å using the following equation

$$W_{\rm C} = \frac{h^2}{2\pi c}(1/2m^3\pi k)^{1/2}\frac{\lambda^2 N}{Z^2\sqrt{T}}\left(n_{\rm i}^{*4} + n_{\rm f}^{*4}\right), \quad (1)$$

where h is Planck's constant, c is the speed of light, m is the mass of perturber, $Z-1$ is the ionic charge, N electron density in m^{-3}, T is the temperature in K, λ is the wavelength in Å, and n^* is the effective principal quantum number. The indices i and f denote the initial level and the final level of the transition.

Table 2 is organized as follows: in the first two columns, we give the transition and the wavelength taken from Kurucz data base. Our electron impact Stark width ($W_{\rm e}$) calculated using SCP approach is presented in Å in column three and in s^{-1} in column four. In column five, we give the Stark width ($W_{\rm c1}$) calculated using Cowley's formula

Table 1. Our calculated wavelengths, weighted oscillator strengths and transition probabilities in s^{-1} for Ni v ion compared with the values taken from Kurucz data base (2023).

Lower level (i)	Upper level (j)	λ (Å) This work	λ (Å) Kurucz	gf This work	gf Kurucz	A_{ji} This work	A_{ji} Kurucz
$(^2D2)\ 4s\ ^1D_2$	$(^2G1)\ 4p\ ^1F^o_3$	1089.493	1109.654	2.54×10^{-1}	2.20×10^{-1}	1.965×10^{8}	1.764×10^{8}
$(^2H)\ 4s\ ^3H_5$	$(^2F2)\ 4p\ ^3G^o_4$	1123.077	1120.883	6.41×10^{-1}	7.26×10^{-1}	3.771×10^{8}	4.283×10^{8}
$(^2H)\ 4s\ ^3H_6$	$(^2F2)\ 4p\ ^3G^o_5$	1123.483	1124.297	8.30×10^{-1}	1.00	3.985×10^{8}	4.808×10^{8}
$(^2H)\ 4s\ ^1H_5$	$(^2H)\ 4p\ ^1G^o_4$	1153.721	1152.675	8.69×10^{-1}	1.07	4.834×10^{8}	5.977×10^{8}
$(^2D1)\ 4s\ ^3D_3$	$(^2D1)\ 4p\ ^3P^o_2$	1187.075	1170.267	7.43×10^{-1}	7.03×10^{-1}	7.038×10^{8}	6.848×10^{8}
$(^2D1)\ 4s\ ^3D_2$	$(^2D1)\ 4p\ ^3P^o_2$	1188.067	1171.121	2.03×10^{-1}	1.98×10^{-1}	1.915×10^{8}	1.923×10^{8}
$(^4P)\ 4s\ ^5P_3$	$(^4D)\ 4p\ ^5D^o_4$	1198.377	1178.919	1.01	9.25×10^{-1}	5.248×10^{8}	4.931×10^{8}
$(^4P)\ 4s\ ^5P_2$	$(^4D)\ 4p\ ^5D^o_3$	1202.199	1185.950	6.62×10^{-1}	5.36×10^{-1}	4.361×10^{8}	3.630×10^{8}
$(^4P)\ 4s\ ^5P_1$	$(^4D)\ 4p\ ^3P^o_0$	1202.497	1191.073	1.42×10^{-1}	1.22×10^{-1}	6.562×10^{8}	5.731×10^{8}
$(^2D1)\ 4s\ ^3D_3$	$(^2D1)\ 4p\ ^3D^o_3$	1214.053	1197.385	1.17	1.15	8.463×10^{8}	7.613×10^{8}
$(^2D1)\ 4s\ ^3D_2$	$(^2D1)\ 4p\ ^3D^o_3$	1215.091	1198.279	8.13×10^{-1}	8.36×10^{-1}	5.249×10^{8}	5.545×10^{8}
$(^2H)\ 4s\ ^3H_6$	$(^2G2)\ 4p\ ^3H^o_6$	1206.831	1199.403	1.46	1.56	5.140×10^{8}	5.562×10^{8}
$(^2D2)\ 4s\ ^3D_1$	$(^2D2)\ 4p\ ^3P^o_1$	1209.766	1201.077	3.39×10^{-1}	3.25×10^{-1}	5.146×10^{8}	5.010×10^{8}
$(^2D2)\ 4s\ ^3D_2$	$(^2D2)\ 4p\ ^3P^o_1$	1210.505	1201.579	4.60×10^{-1}	4.13×10^{-1}	6.977×10^{8}	6.361×10^{8}
$(^2D2)\ 4s\ ^3D_1$	$(^2D2)\ 4p\ ^3P^o_0$	1209.722	1201.644	2.79×10^{-1}	2.61×10^{-1}	1.273×10^{9}	1.204×10^{9}
$(^2F2)\ 4s\ ^3F_3$	$(^2F2)\ 4p\ ^3G^o_4$	1233.301	1202.029	1.80	1.35	8.773×10^{8}	6.919×10^{8}
$(^2D2)\ 4s\ ^3D_2$	$(^2D2)\ 4p\ ^3P^o_2$	1211.485	1202.260	4.03×10^{-1}	3.82×10^{-1}	3.658×10^{8}	3.525×10^{8}
$(^2D2)\ 4s\ ^3D_3$	$(^2D2)\ 4p\ ^3P^o_2$	1212.826	1203.274	8.13×10^{-1}	7.16×10^{-1}	7.376×10^{8}	6.598×10^{8}
$(^2F2)\ 4s\ ^1F_3$	$(^2F2)\ 4p\ ^1F^o_3$	1210.620	1203.765	2.07	1.90	1.346×10^{9}	1.247×10^{9}
$(^2H)\ 4s\ ^3H_4$	$(^2H)\ 4p\ ^3H^o_4$	1343.503	1205.303	1.23	9.93×10^{-1}	5.034×10^{8}	5.066×10^{8}
$(^2H)\ 4s\ ^3H_5$	$(^2H)\ 4p\ ^3H^o_5$	1215.373	1207.345	1.17	1.16	4.790×10^{8}	4.809×10^{8}
$(^2F2)\ 4s\ ^3F_3$	$(^2F2)\ 4p\ ^3D^o_2$	1234.252	1209.608	1.04	9.31×10^{-1}	9.130×10^{8}	8.489×10^{8}
$(^4F)\ 4s\ ^5F_5$	$(^4F)\ 4p\ ^5D^o_4$	1225.562	1209.747	8.65×10^{-1}	7.26×10^{-1}	4.270×10^{8}	3.677×10^{8}
$(^4F)\ 4s\ ^5F_4$	$(^4F)\ 4p\ ^5D^o_4$	1226.532	1210.381	1.24	1.27	6.131×10^{8}	6.413×10^{8}
$(^2D1)\ 4s\ ^3D_2$	$(^2D1)\ 4p\ ^3D^o_2$	1226.687	1211.437	6.38×10^{-1}	5.51×10^{-1}	5.660×10^{8}	5.007×10^{8}
$(^4D)\ 4s\ ^5D_2$	$(^4D)\ 4p\ ^5P^o_2$	1223.952	1212.781	5.79×10^{-1}	5.86×10^{-1}	5.156×10^{8}	5.316×10^{8}
$(^4F)\ 4s\ ^5F_1$	$(^4F)\ 4p\ ^5D^o_0$	1235.454	1214.391	2.48×10^{-1}	2.45×10^{-1}	1.082×10^{9}	1.110×10^{9}
$(^2F2)\ 4s\ ^3F_2$	$(^2F2)\ 4p\ ^3D^o_1$	1236.846	1215.107	7.40×10^{-1}	6.27×10^{-1}	1.074×10^{9}	9.436×10^{8}
$(^2G2)\ 4s\ ^3G_5$	$(^2G2)\ 4p\ ^3H^o_6$	1236.002	1215.277	1.37	1.09	4.618×10^{8}	3.774×10^{8}
$(^2D2)\ 4s\ ^1D_2$	$(^2D2)\ 4p\ ^1D^o_2$	1253.201	1230.435	1.45	1.32	1.234×10^{9}	1.167×10^{9}
$(^2D2)\ 4s\ ^3D_3$	$(^2D2)\ 4p\ ^3F^o_4$	1249.074	1232.694	2.70	2.53	1.284×10^{9}	1.233×10^{9}
$(^2H)\ 4s\ ^1H_5$	$(^2H)\ 4p\ ^1H^o_5$	1261.763	1232.807	2.05	1.94	7.800×10^{8}	7.744×10^{8}
$(^4F)\ 4s\ ^5F_5$	$(^4F)\ 4p\ ^5F^o_5$	1246.244	1233.257	1.83	1.77	7.168×10^{8}	7.041×10^{8}
$(^4G)\ 4s\ ^5G_2$	$(^4G)\ 4p\ ^5F^o_1$	1245.242	1234.393	7.89×10^{-1}	6.67×10^{-1}	1.131×10^{9}	9.730×10^{8}
$(^4F)\ 4s\ ^5F_2$	$(^2F1)\ 4p\ ^3D^o_1$	1241.910	1236.277	4.41×10^{-1}	5.47×10^{-1}	6.347×10^{8}	7.957×10^{8}
$(^2G1)\ 4s\ ^1G_4$	$(^2G1)\ 4p\ ^1F^o_3$	1247.067	1236.702	1.86	1.70	1.137×10^{9}	1.058×10^{9}
$(^4D)\ 4s\ ^5D_4$	$(^4D)\ 4p\ ^5D^o_4$	1256.649	1236.706	1.61	1.37	7.549×10^{8}	6.637×10^{8}
$(^4F)\ 4s\ ^5F_5$	$(^4F)\ 4p\ ^5G^o_6$	1261.664	1239.552	3.94	1.23	1.269×10^{9}	4.099×10^{8}
$(^4F)\ 4s\ ^3F_4$	$(^2G2)\ 4p\ ^3H^o_5$	1266.784	1241.047	2.41×10^{-1}	2.89×10^{-1}	9.154×10^{7}	1.133×10^{8}
$(^4F)\ 4s\ ^5F_3$	$(^4F)\ 4p\ ^5F^o_2$	1251.742	1241.319	7.14×10^{-1}	9.10×10^{-1}	6.086×10^{8}	7.878×10^{8}
$(^2I)\ 4s\ ^3I_5$	$(^2I)\ 4p\ ^3H^o_4$	1247.161	1241.627	2.75	2.20	1.310×10^{9}	1.059×10^{9}
$(^4F)\ 4s\ ^5F_5$	$(^4F)\ 4p\ ^5F^o_4$	1254.470	1241.972	1.11	1.30	5.237×10^{8}	6.232×10^{8}
$(^2I)\ 4s\ ^3I_6$	$(^2I)\ 4p\ ^3H^o_5$	1249.100	1242.071	2.53	2.42	9.836×10^{8}	9.516×10^{8}
$(^4D)\ 4s\ ^5D_3$	$(^4D)\ 4p\ ^5D^o_2$	1257.885	1243.504	6.81×10^{-1}	5.70×10^{-1}	5.736×10^{8}	4.919×10^{8}
$(^4D)\ 4s\ ^5D_4$	$(^4D)\ 4p\ ^5D^o_3$	1258.635	1244.027	5.98×10^{-1}	4.53×10^{-1}	3.600×10^{8}	2.788×10^{8}
$(^4F)\ 4s\ ^5F_5$	$(^2I)\ 4p\ ^1I^o_6$	1261.664	1245.176	3.94	2.58	1.269×10^{9}	8.545×10^{8}
$(^4D)\ 4s\ ^3D_2$	$(^4D)\ 4p\ ^3P^o_1$	1254.296	1246.547	4.16×10^{-1}	3.99×10^{-1}	5.877×10^{8}	5.709×10^{8}
$(^2D2)\ 4s\ ^3D_1$	$(^2D2)\ 4p\ ^3D^o_2$	1265.052	1246.808	9.46×10^{-1}	1.01	7.892×10^{8}	8.641×10^{8}
$(^2D2)\ 4s\ ^1D_2$	$(^2D2)\ 4p\ ^1P^o_1$	1257.008	1246.821	7.38×10^{-1}	6.73×10^{-1}	1.038×10^{9}	9.625×10^{8}
$(^4G)\ 4s\ ^5G_5$	$(^4G)\ 4p\ ^5F^o_4$	1257.015	1249.522	1.87	1.45	8.800×10^{8}	6.893×10^{8}
$(^4D)\ 4s\ ^5D_3$	$(^4D)\ 4p\ ^5D^o_3$	1265.097	1250.344	5.90×10^{-1}	5.48×10^{-1}	3.514×10^{8}	3.342×10^{8}
$(^4G)\ 4s\ ^5G_6$	$(^4G)\ 4p\ ^5H^o_7$	1268.790	1250.388	4.81	4.59	1.328×10^{9}	1.306×10^{9}
$(^2H)\ 4s\ ^3H_5$	$(^2G2)\ 4p\ ^3F^o_4$	1241.805	1250.403	3.13×10^{-1}	4.18×10^{-1}	1.504×10^{8}	1.981×10^{8}
$(^4G)\ 4s\ ^5G_6$	$(^4G)\ 4p\ ^5F^o_5$	1262.287	1252.183	2.61	2.13	9.927×10^{8}	8.249×10^{8}
$(^2I)\ 4s\ ^3I_6$	$(^2I)\ 4p\ ^3H^o_6$	1260.812	1252.267	8.45×10^{-1}	1.03	2.725×10^{8}	3.379×10^{8}
$(^2I)\ 4s\ ^3I_7$	$(^2I)\ 4p\ ^3H^o_6$	1262.399	1252.756	3.04	2.54	9.785×10^{8}	8.288×10^{8}
$(^2D2)\ 4s\ ^3D_1$	$(^2D2)\ 4p\ ^3D^o_1$	1272.638	1253.489	5.71×10^{-1}	5.28×10^{-1}	7.850×10^{8}	7.478×10^{8}
$(^4F)\ 4s\ ^3F_2$	$(^4F)\ 4p\ ^3D^o_1$	1268.006	1254.417	7.10×10^{-1}	6.53×10^{-1}	9.813×10^{8}	9.288×10^{8}
$(^2G1)\ 4s\ ^1G_4$	$(^2G1)\ 4p\ ^1G^o_4$	1272.363	1256.905	2.74	2.56	1.254×10^{9}	1.203×10^{9}
$(^4G)\ 4s\ ^5G_5$	$(^4G)\ 4p\ ^5H^o_6$	1274.346	1257.626	4.07	3.85	1.287×10^{9}	1.248×10^{9}
$(^2I)\ 4s\ ^3I_5$	$(^2I)\ 4p\ ^1H^o_5$	1262.761	1259.587	9.12×10^{-1}	1.03	3.471×10^{8}	3.947×10^{8}
$(^4F)\ 4s\ ^5F_5$	$(^4F)\ 4p\ ^5G^o_5$	1273.670	1259.722	9.83×10^{-1}	9.44×10^{-1}	3.671×10^{8}	3.607×10^{8}

Table 1 – *continued*

Lower level (*i*)	Upper level (*j*)	λ (Å) This work	λ (Å) Kurucz	*gf* This work	*gf* Kurucz	A_{ji} This work	A_{ji} Kurucz
(^{4}D) 4s ^{5}D$_4$	(^{4}D) 4p ^{5}F$^o_5$	1276.551	1261.760	3.21	3.01	1.194×10^9	1.145×10^9
(^{2}G1) 4s ^{3}G$_4$	(^{2}G1) 4p ^{3}F$^o_3$	1271.903	1262.539	1.65	1.64	9.740×10^8	9.830×10^8
(^{2}D1) 4s ^{1}D$_2$	(^{2}D1) 4p ^{1}D$^o_2$	1279.029	1262.550	9.68×10^{-1}	9.10×10^{-1}	7.894×10^8	7.615×10^8
(^{2}H) 4s ^{3}H$_6$	(^{2}H) 4p ^{3}I$^o_7$	1282.343	1265.671	4.69	4.43	1.269×10^9	1.229×10^9
(^{4}F) 4s ^{5}F$_3$	(^{4}F) 4p ^{5}G$^o_4$	1280.534	1265.725	1.19	1.18	5.358×10^8	5.473×10^8
(^{4}G) 4s ^{5}G$_4$	(^{4}G) 4p ^{5}H$^o_5$	1281.070	1266.408	3.25	2.86	1.202×10^9	1.080×10^9
(^{4}P) 4s ^{5}P$_1$	(^{4}P) 4p ^{5}P$^o_2$	1280.561	1266.876	8.90×10^{-1}	8.91×10^{-1}	7.242×10^8	7.408×10^8
(^{2}I) 4s ^{3}I$_6$	(^{2}I) 4p ^{3}I$^o_7$	1281.734	1267.291	2.21	2.14	5.985×10^8	5.919×10^8
(^{2}I) 4s ^{3}I$_7$	(^{2}I) 4p ^{3}I$^o_7$	1283.374	1267.802	2.54	2.35	6.853×10^8	6.500×10^8
(^{2}G1) 4s ^{3}G$_4$	(^{2}G1) 4p ^{3}H$^o_5$	1283.858	1268.873	2.33	2.05	8.555×10^8	7.707×10^8
(^{2}H) 4s ^{3}H$_5$	(^{2}H) 4p ^{3}I$^o_6$	1285.979	1269.387	2.38	1.76	7.372×10^8	5.610×10^8
(^{2}I) 4s ^{3}I$_7$	(^{2}I) 4p ^{3}K$^o_8$	1288.962	1270.677	5.41	5.15	1.278×10^9	1.252×10^9
(^{4}G) 4s ^{5}G$_3$	(^{4}G) 4p ^{5}H$^o_4$	1287.258	1273.204	2.69	2.48	1.203×10^9	1.135×10^9
(^{4}P) 4s ^{5}P$_2$	(^{4}P) 4p ^{5}P$^o_3$	1286.450	1273.827	1.06	1.02	6.113×10^8	5.954×10^8
(^{4}F) 4s ^{5}F$_2$	(^{4}F) 4p ^{5}G$^o_3$	1288.419	1274.264	1.27	1.00	7.271×10^8	5.855×10^8
(^{4}D) 4s ^{5}D$_3$	(^{4}D) 4p ^{5}F$^o_4$	1289.834	1276.428	2.25	2.05	1.003×10^9	9.309×10^8
(^{6}S) 4s ^{7}S$_3$	(^{6}S) 4p ^{7}P$^o_2$	1287.252	1276.958	1.57	1.49	1.262×10^9	1.218×10^9
(^{4}G) 4s ^{5}G$_2$	(^{4}G) 4p ^{5}H$^o_3$	1293.210	1279.720	2.12	2.00	1.207×10^9	1.161×10^9
(^{2}I) 4s ^{3}I$_6$	(^{2}I) 4p ^{3}I$^o_6$	1293.367	1282.201	1.88	1.46	5.763×10^8	4.563×10^8
(^{2}I) 4s ^{3}I$_5$	(^{2}I) 4p ^{3}I$^o_6$	1292.415	1282.270	1.35	1.27	4.145×10^8	3.956×10^8
(^{2}I) 4s ^{3}I$_7$	(^{2}I) 4p ^{3}I$^o_6$	1295.037	1282.724	7.85×10^{-1}	1.01	2.401×10^8	3.147×10^8
(^{2}S) 4s ^{3}S$_1$	(^{2}S) 4p ^{3}P$^o_2$	1301.477	1285.793	1.27	1.16	1.001×10^9	9.393×10^8
(^{2}D3) 4s ^{3}D$_3$	(^{2}D3) 4p ^{3}F$^o_4$	1301.610	1287.553	1.40	1.32	6.127×10^8	5.880×10^8
(^{4}D) 4s ^{5}D$_1$	(^{4}D) 4p ^{5}F$^o_2$	1300.660	1287.808	8.09×10^{-1}	7.31×10^{-1}	6.376×10^8	5.895×10^8
(^{2}G2) 4s ^{3}G$_5$	(^{2}H) 4p ^{3}I$^o_6$	1327.435	1298.738	1.49	1.85	4.322×10^8	5.612×10^8
(^{6}S) 4s ^{5}S$_2$	(^{6}S) 4p ^{5}P$^o_1$	1314.483	1300.979	9.55×10^{-1}	8.95×10^{-1}	1.227×10^9	1.176×10^9
(^{2}F1) 4s ^{3}F$_2$	(^{2}F1) 4p ^{3}G$^o_3$	1321.210	1303.326	9.20×10^{-1}	1.15	5.023×10^8	6.441×10^8
(^{2}I) 4s ^{3}I$_7$	(^{2}I) 4p ^{3}K$^o_7$	1317.314	1306.238	2.00	1.92	5.137×10^8	5.012×10^8
(^{4}G) 4s ^{5}G$_6$	(^{4}G) 4p ^{5}G$^o_6$	1313.133	1306.624	3.94	3.67	1.170×10^9	1.104×10^9
(^{6}S) 4s ^{5}S$_2$	(^{6}S) 4p ^{5}P$^o_2$	1320.665	1307.603	1.57	1.47	1.202×10^9	1.149×10^9
(^{4}G) 4s ^{5}G$_6$	(^{4}G) 4p ^{5}G$^o_5$	1316.544	1309.653	5.25×10^{-1}	5.08×10^{-1}	1.760×10^8	1.809×10^8
(^{4}F) 4s ^{3}F$_2$	(^{4}F) 4p ^{3}G$^o_3$	1324.771	1309.689	9.89×10^{-1}	8.36×10^{-1}	5.369×10^8	4.642×10^8
(^{4}F) 4s ^{3}F$_4$	(^{4}F) 4p ^{3}G$^o_5$	1326.158	1310.252	2.06	1.63	7.090×10^8	5.741×10^8
(^{4}G) 4s ^{5}G$_5$	(^{4}G) 4p ^{5}G$^o_5$	1316.841	1311.106	2.86	2.65	1.000×10^9	9.342×10^8
(^{2}H) 4s ^{3}H$_5$	(^{2}H) 4p ^{3}H$^o_6$	1321.164	1311.560	7.96×10^{-1}	8.18×10^{-1}	2.341×10^8	2.441×10^8
(^{2}I) 4s ^{3}I$_6$	(^{2}I) 4p ^{3}K$^o_6$	1323.586	1312.646	1.33	1.31	3.900×10^8	3.889×10^8
(^{4}G) 4s ^{3}G$_3$	(^{4}G) 4p ^{5}G$^o_3$	1319.175	1314.330	1.58	1.48	8.686×10^8	8.159×10^8
(^{4}G) 4s ^{5}G$_2$	(^{4}G) 4p ^{5}G$^o_2$	1319.047	1314.682	1.17	1.09	9.001×10^8	8.385×10^8
(^{2}D3) 4s ^{3}D$_3$	(^{2}D3) 4p ^{3}F$^o_3$	1326.593	1314.992	8.59×10^{-1}	8.07×10^{-1}	4.656×10^8	4.448×10^8
(^{4}D) 4s ^{3}D$_1$	(^{4}D) 4p ^{3}F$^o_2$	1325.804	1315.653	1.10	1.02	8.358×10^8	7.832×10^8
(^{4}D) 4s ^{3}D$_2$	(^{4}D) 4p ^{3}F$^o_2$	1327.800	1316.890	3.17×10^{-1}	3.08×10^{-1}	2.398×10^8	2.366×10^8
(^{2}D3) 4s ^{3}D$_2$	(^{2}D3) 4p ^{3}F$^o_3$	1326.971	1316.892	6.87×10^{-1}	7.19×10^{-1}	3.717×10^8	3.953×10^8
(^{2}I) 4s ^{1}I$_6$	(^{2}I) 4p ^{1}K$^o_7$	1334.234	1317.447	4.40	4.12	1.098×10^9	1.056×10^9
(^{6}S) 4s ^{5}S$_2$	(^{6}S) 4p ^{5}P$^o_3$	1330.722	1318.515	2.17	2.03	1.168×10^9	1.111×10^9
(^{2}F1) 4s ^{3}F$_3$	(^{2}F1) 4p ^{1}G$^o_4$	1334.742	1323.553	5.25×10^{-1}	5.83×10^{-1}	2.183×10^8	2.468×10^8
(^{2}H) 4s ^{3}H$_6$	(^{2}H) 4p ^{3}H$^o_6$	1329.470	1323.562	2.28	1.99	6.608×10^8	5.830×10^8
(^{4}G) 4s ^{3}G$_3$	(^{4}G) 4p ^{3}H$^o_4$	1339.956	1323.977	2.22	2.47	9.147×10^8	1.043×10^9
(^{4}P) 4s ^{5}P$_2$	(^{4}P) 4p ^{5}D$^o_2$	1325.669	1324.000	6.95×10^{-1}	6.04×10^{-1}	5.278×10^8	4.596×10^8
(^{4}P) 4s ^{5}P$_1$	(^{4}P) 4p ^{5}D$^o_1$	1333.618	1328.025	4.21×10^{-1}	4.01×10^{-1}	5.256×10^8	5.124×10^8
(^{4}G) 4s ^{3}G$_4$	(^{4}G) 4p ^{3}H$^o_5$	1344.944	1329.358	3.18	2.97	1.067×10^9	1.020×10^9
(^{2}I) 4s ^{1}I$_6$	(^{2}I) 4p ^{1}H$^o_5$	1338.529	1333.958	1.95	1.73	6.598×10^8	5.881×10^8
(^{2}H) 4s ^{3}H$_6$	(^{2}H) 4p ^{3}G$^o_5$	1331.290	1334.169	1.82	1.79	6.244×10^8	6.114×10^8
(^{4}G) 4s ^{3}G$_5$	(^{4}G) 4p ^{3}H$^o_6$	1351.158	1336.136	3.84	3.61	1.078×10^9	1.036×10^9
(^{4}D) 4s ^{5}D$_4$	(^{4}P) 4p ^{5}P$^o_3$	1351.287	1341.074	7.87×10^{-1}	7.40×10^{-1}	4.107×10^8	3.919×10^8
(^{4}G) 4s ^{3}G$_5$	(^{4}G) 4p ^{3}F$^o_4$	1349.698	1342.176	2.16	2.21	8.788×10^8	9.105×10^8
(^{4}G) 4s ^{3}G$_3$	(^{4}G) 4p ^{3}F$^o_2$	1356.602	1351.412	1.28	1.26	9.294×10^9	9.174×10^9

without the contribution of the lower level. In column six, we present the width (W_{c2}) obtained using Cowley's formula (equation (1)) with the contribution of the lower level. Finally, in the two last columns, the ratios W_e/W_{C1} and W_e/W_{C2} are given. After introducing the lower-level contribution, the values obtained using Cowley's formula increase by a factor 0.63 on average. The values W_{C1} agree with the values obtained using SCP method within 70 per cent on average. The largest disagreement is found for the transition (^{6}S) 4s ^{5}S$_2$–(^{6}S)

Table 2. Electron impact Stark widths calculated using SCP approach (Sahal-Bréchot 1969a, b; Sahal-Bréchot, Dimitrijević & Nessib 2014) (W_e) and Cowley formula (Cowley 1971) (W_{C1} and W_{C2}). W_{C1}: calculated without contribution of lower level, W_{C2}: calculated with contribution of lower level. Stark widths are calculated at the temperature 10 kK and electron density 10^{17} cm^{-3}. Wavelengths are taken from Kurucz data base (2023).

Transition	Wavelength (Å)	W_e (pm)	W_e (10^{11} s^{-1})	W_{C1} (pm)	W_{C2} (pm)	W_e/W_{C1}	W_e/W_{C2}
(^{2}D2) 4s ^{1}D$_2$–(^{2}D2) 4p ^{1}D$^o_2$	1230.435	2.40	2.98	1.88	2.78	1.28	0.86
(^{2}H) 4s ^{1}H$_5$–(^{2}H) 4p ^{1}H$^o_5$	1232.807	2.30	2.85	1.61	2.58	1.43	0.89
(^{4}F) 4s ^{5}F$_5$–(^{4}F) 4p ^{5}F$^o_5$	1233.257	2.16	2.67	1.48	2.40	1.46	0.90
(^{4}G) 4s ^{5}G$_2$–(^{4}G) 4p ^{5}F$^o_1$	1234.393	2.16	2.67	1.25	2.06	1.73	1.05
(^{4}F) 4s ^{5}F$_2$–(^{2}F1) 4p ^{3}D$^o_1$	1236.277	2.10	2.59	1.49	2.41	1.40	0.87
(^{4}F) 4s ^{5}F$_5$–(^{4}F) 4p ^{5}G$^o_6$	1239.552	2.24	2.75	1.49	2.42	1.50	0.89
(^{2}I) 4s ^{3}I$_5$–(^{2}I) 4p ^{3}H$^o_4$	1241.627	2.28	2.79	1.45	2.35	1.57	0.97
(^{4}D) 4s ^{5}D$_3$–(^{4}D) 4p ^{5}D$^o_2$	1243.504	2.06	2.51	1.34	2.19	1.54	0.94
(^{4}D) 4s ^{5}D$_4$–(^{4}D) 4p ^{5}D$^o_3$	1244.027	2.10	2.55	1.34	2.18	1.57	0.96
(^{4}F) 4s ^{5}F$_5$–(^{2}I) 4p ^{1}I$^o_6$	1245.176	2.29	2.78	1.51	2.44	1.52	0.94
(^{4}G) 4s ^{5}G$_5$–(^{4}G) 4p ^{5}H$^o_6$	1257.626	2.39	2.85	1.29	2.12	1.85	1.12
(^{4}D) 4s ^{5}D$_4$–(^{4}D) 4p ^{5}F$^o_5$	1261.760	2.29	2.71	1.36	2.24	1.68	1.02
(^{4}G) 4s ^{5}G$_3$–(^{4}G) 4p ^{5}H$^o_4$	1273.204	2.34	2.72	1.31	2.16	1.79	1.08
(^{4}G) 4s ^{5}G$_2$–(^{4}G) 4p ^{5}H$^o_3$	1279.720	2.48	2.86	1.33	2.19	1.86	1.13
(^{6}S) 4s ^{5}S$_2$–(^{6}S) 4p ^{5}P$^o_1$	1300.979	2.52	2.81	1.14	1.91	2.21	1.32
(^{6}S) 4s ^{5}S$_2$–(^{6}S) 4p ^{5}P$^o_2$	1307.603	2.55	2.81	1.15	1.93	2.22	1.32
(^{6}S) 4s ^{5}S$_2$–(^{6}S) 4p ^{5}P$^o_3$	1318.515	2.59	2.81	1.16	1.96	2.23	1.32
(^{4}G) 4s ^{3}G$_5$–(^{4}G) 4p ^{3}H$^o_6$	1336.136	2.57	2.71	1.50	2.48	1.71	1.04
(^{4}G) 4s ^{3}G$_5$–(^{4}G) 4p ^{3}F$^o_4$	1342.176	2.61	2.73	1.50	2.50	1.74	1.04

Table 3. Fitting parameters a, b, and c for equation (2). R^2 is the root mean square of the fitting.

Transition	Wavelength (Å)	a	b	c	R^2
(^{2}D2) 4s ^{1}D$_2$–(^{2}D2) 4p ^{1}D$^o_2$	1230.435	2.83093	−1.52703	0.10790	0.99995
(^{2}H) 4s ^{1}H$_5$–(^{2}H) 4p ^{1}H$^o_5$	1232.807	2.42652	−1.38506	0.09431	0.99995
(^{4}F) 4s ^{5}F$_5$–(^{4}F) 4p ^{5}F$^o_5$	1233.257	2.62868	−1.46247	0.10162	0.99993
(^{4}G) 4s ^{5}G$_2$–(^{4}G) 4p ^{5}F$^o_1$	1234.393	2.62829	−1.45782	0.10023	0.99996
(^{4}F) 4s ^{5}F$_2$–(^{2}F1) 4p ^{3}D$^o_1$	1236.277	2.46140	−1.39898	0.09507	0.99996
(^{4}F) 4s ^{5}F$_5$–(^{4}F) 4p ^{5}G$^o_6$	1239.552	2.56622	−1.43769	0.09958	0.99995
(^{2}I) 4s ^{3}I$_5$–(^{2}I) 4p ^{3}H$^o_4$	1241.627	2.74214	−1.49406	0.10398	0.99998
(^{4}D) 4s ^{5}D$_3$–(^{4}D) 4p ^{5}D$^o_2$	1243.504	2.47098	−1.40563	0.09579	0.99996
(^{4}D) 4s ^{5}D$_4$–(^{4}D) 4p ^{5}D$^o_3$	1244.027	2.47156	−1.40347	0.09540	0.99996
(^{4}F) 4s ^{5}F$_5$–(^{2}I) 4p ^{1}I$^o_6$	1245.176	2.47975	−1.40421	0.09657	0.99990
(^{4}G) 4s ^{5}G$_5$–(^{4}G) 4p ^{5}H$^o_6$	1257.626	2.77926	−1.50574	0.10516	0.99996
(^{4}D) 4s ^{5}D$_4$–(^{4}D) 4p ^{5}F$^o_5$	1261.760	2.64213	−1.46061	0.10139	0.99998
(^{4}G) 4s ^{5}G$_3$–(^{4}G) 4p ^{5}H$^o_4$	1273.204	2.64492	−1.45895	0.10128	0.99998
(^{4}G) 4s ^{5}G$_2$–(^{4}G) 4p ^{5}H$^o_3$	1279.720	2.86620	−1.53190	0.10751	0.99999
(^{6}S) 4s ^{5}S$_2$–(^{6}S) 4p ^{5}P$^o_1$	1300.979	2.70089	−1.45964	0.10067	0.99997
(^{6}S) 4s ^{5}S$_2$–(^{6}S) 4p ^{5}P$^o_2$	1307.603	2.69684	−1.45623	0.10030	0.99997
(^{6}S) 4s ^{5}S$_2$–(^{6}S) 4p ^{5}P$^o_3$	1318.515	2.70183	−1.45554	0.10026	0.99996
(^{4}G) 4s ^{3}G$_5$–(^{4}G) 4p ^{3}H$^o_6$	1336.136	2.43458	−1.36354	0.09263	0.99992
(^{4}G) 4s ^{3}G$_5$–(^{4}G) 4p ^{3}F$^o_4$	1342.176	2.79071	−1.48958	0.10364	0.99997

4p ^{5}P$^o_3$ for which the ratio W_e/W_{C1} is equal 2.23. After introducing the lower level contribution, the agreement between the estimates obtained using Cowley's formula and the results obtained using SCP approach is improved and the differences between the values W_e and W_{C2} do not exceed 32 per cent. Electron impact Stark widths presented in angular frequency unit show that the greatest value is 1.19 times greater than the smallest one.

It is more convenient for astrophysical purposes to use Stark broadening parameters fitted with temperature using the equation obtained in Sahal-Bréchot, Dimitrijević & Ben Nessib (2011):

$$\log W_e(T) = a + b \times \log T + c \times [\log T]^2, \quad (2)$$

where W_e is the electron impact Stark width in Å obtained using SCP approach, T is the temperature in K and a, b, c are the fitting parameters. In Al-Towyan et al. (2016), several fitting formulas have been compared for Cr I spectral lines, and it was shown that the logarithmic formula (equation (2)) gives better results. Our fitting parameters for Ni V spectral lines are shown in Table 3 for the electron density 10^{17} cm^{-3} and temperatures from 50 to 600 kK.

4 LARGE SCALE RESULTS

Our large-scale results for 120 ultraviolet spectral lines of Ni V ion are presented in Tables S_1, S_2, and S_3 for the perturber densities 10^{17}, 10^{18}, and 10^{19} cm^{-3}, respectively. The tables are available online as supplementary data. The range of temperature from 50 to 600 kK. Taking into account the most important perturbers in white dwarf atmospheres, our Stark widths and shifts are calculated for collisions with electrons and also with the positive ions: H^+, He^+, and He^{++}. We give in Table 4 an example of two transitions showing

Table 4. Electron-, proton- singly and doubly charged helium-impact Stark broadening parameters for 4s–4p spectral lines of Ni V calculated using SCP approach (Sahal-Bréchot 1969a, b; Sahal-Bréchot, Dimitrijević & Nessib 2014) for aperturber density of 10^{17} cm^{-3} and temperature of 50 to 600 kK. The needed atomic data are calculated using Cowancode (Cowan 1981). W_e: electron-impact full Stark width at half maximum, d_e: electron-impact Stark shift, W_{H^+}: proton-impact full Stark width at half maximum, d_{H^+}: proton-impact Stark shift, W_{He^+}: singly charged helium-impact full Stark width at half maximum, d_{He^+}: singly charged helium-impact Stark shift. $W_{He^{++}}$: doubly charged helium-impact full Stark width at half maximum, $d_{He^{++}}$: doubly charged helium-impact Stark shift. All wavelengths aretaken from Kurucz data base (2023). This table illustrates the form and content of additional data presented in Tables S_1, S_2, and S_3.

Transition	T (kK)	W_e (Å)	d_e (Å)	W_{H+} (Å)	d_{H+} (Å)	W_{He+} (Å)	d_{He+} (Å)	W_{He++} (Å)	d_{He++} (Å)
(^{2}D2) 4s ^{1}D$_2$–(^{2}D2) 4p ^{1}D$^o_2$	50.	0.109E-01	−0.135E-03	0.475E-03	−0.662E-04	0.674E-03	−0.650E-04	0.937E-03	−0.129E-03
1230.435 Å	100.	0.785E-02	−0.177E-03	0.770E-03	−0.123E-03	0.962E-03	−0.114E-03	0.153E-02	−0.245E-03
C = 0.87E + 20	200.	0.586E-02	−0.183E-03	0.106E-02	−0.193E-03	0.115E-02	−0.166E-03	0.210E-02	−0.388E-03
	300.	0.505E-02	−0.202E-03	0.114E-02	−0.234E-03	0.123E-02	−0.201E-03	0.228E-02	−0.470E-03
	400.	0.460E-02	−0.196E-03	0.120E-02	−0.265E-03	0.129E-02	−0.221E-03	0.241E-02	−0.534E-03
	600.	0.408E-02	−0.184E-03	0.129E-02	−0.297E-03	0.137E-02	−0.245E-03	0.258E-02	−0.598E-03
(^{4}F) 4s ^{5}F$_5$–(^{4}F) 4p ^{5}G$^o_6$	50.	0.102E-01	−0.111E-03	0.310E-03	−0.572E-04	0.455E-03	−0.564E-04	0.609E-03	−0.111E-03
1239.552 Å	100.	0.739E-02	−0.148E-03	0.543E-03	−0.107E-03	0.678E-03	−0.994E-04	0.107E-02	−0.213E-03
C = 0.82E + 20	200.	0.553E-02	−0.151E-03	0.767E-03	−0.172E-03	0.858E-03	−0.148E-03	0.152E-02	−0.345E-03
	300.	0.477E-02	−0.167E-03	0.858E-03	−0.208E-03	0.927E-03	−0.180E-03	0.171E-02	−0.418E-03
	400.	0.433E-02	−0.156E-03	0.906E-03	−0.238E-03	0.975E-03	−0.200E-03	0.180E-02	−0.480E-03
	600.	0.384E-02	−0.149E-03	0.975E-03	−0.269E-03	0.103E-02	−0.223E-03	0.195E-02	−0.542E-03

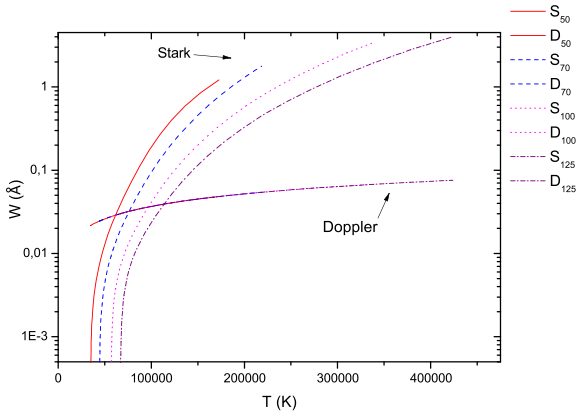

Figure 1. Variation of Stark and Doppler widths with the temperature of the atmospheric layers for Ni V (^{4}D) 4s ^{5}D$_4$–(^{4}D) 4p ^{5}D$^o_3$ (λ = 1244.027 Å) spectral line. Stark (S) and Doppler (D) widths are shown for the atmospheric models (Wesemael et al. 1980) with log g = 8 and effective temperatures from T_{eff} = 50 to 125 kK.

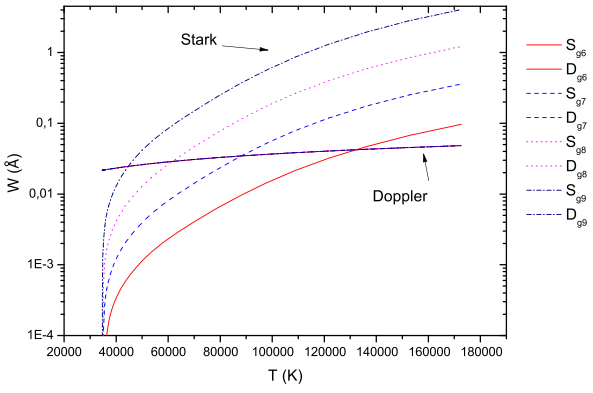

Figure 2. Variation of Stark and Doppler widths with the temperature of the atmospheric layers for Ni V (^{4}D) 4s ^{5}D$_4$–(^{4}D) 4p ^{5}D$^o_3$ (λ = 1244.027 Å) spectral line. Stark (S) and Doppler (D) widths are shown for the atmospheric models (Wesemael et al. 1980) with effective temperature T_{eff} = 50 kK and log g from 6 to 9.

the form of additional data given in Tables S_1, S_2, and S_3. The impact approximation is valid for all values given in Tables S_1, S_2, and S_3 since the collision volume (V) multiplied by the perturber density N is much smaller than one (Sahal-Bréchot, Dimitrijević & Nessib 2014). The asterisk preceding some values of the widths or shifts means that the impact approximation reaches its limit of validity ($0.1 < N V \leq 0.5$). The parameter C (Dimitrijević & Sahal-Bréchot 1984) mentioned in Tables S_1, S_2, and S_3 give an estimation of the maximal perturber density for which the line can be treated as isolated when it is divided by the corresponding Stark width. All wavelengths are taken from the Kurucz data base. The small difference between our calculated wavelengths and the wavelengths of the Kurucz data base is corrected using equation (8) of Hamdi et al. (2013).

All Stark broadening data calculated in this work will be stored in Stark-B data base (Sahal-Bréchot et al. 2015) whose content can be viewed at the following URL: http://stark-b.obspm.fr/.

5 ASTROPHYSICAL IMPLICATIONS

We used our Stark widths calculated for ultraviolet lines of Ni V ion to examine the influence of Stark broadening by electron impacts in the atmospheres of hot DA white dwarfs. Electron impact Stark widths and Doppler widths have been compared as a function of atmospheric layer temperature for different atmospheric models. The atmospheric models used for this purpose are taken from Wesemael et al. (1980). Thermal Doppler width is obtained using equation (21) of Konjević (1999). In Fig. 1, Stark and Doppler widths are compared for Ni V (^{4}D) 4s ^{5}D$_4$–(^{4}D) 4p ^{5}D$^o_3$ (λ = 1244.027 Å) spectral line as a function of atmospheric layer temperature for the atmospheric models with log g = 8, where g is surface gravity, and effective temperatures from T_{eff} = 50 to 125 kK. As we can see from Fig. 1, Stark broadening is dominant for all studied models. The importance of Stark broadening mechanism increases when the effective temperature increases and also when the temperature of the atmospheric layer increases. In Fig. 2, we show the comparison between Stark (S) and Doppler (D) widths for Ni V (^{4}D) 4s ^{5}D$_4$–(^{4}D) 4p ^{5}D$^o_3$ (λ = 1244.027 Å) spectral line for the different temperatures of the atmospheric layers. The comparison is made for the atmospheric models with effective temperature T_{eff} = 50 kK and log g from 6 to 9. Fig. 2 shows that the significance of Stark broadening increases when the surface gravity increases. For the models with log g = 7–9, Stark width is larger than the Doppler

width for all the important atmospheric layers. For the model with log $g = 6$, Stark width becomes larger than Doppler one for the deepest atmospheric layers with a temperature higher than $T \approx 136$ kK.

6 CONCLUSIONS

In this paper, we have calculated Stark broadening data for ultraviolet lines of Ni V ion. Our calculations are performed by combining the SCP approach and HFR approach for atomic structure. The comparison between SCP results and estimations obtained using Cowley's formula show that Cowley's estimations agree with SCP Stark widths when the lower level's contribution is considered.

To make it easier for astrophysical purposes, our electron impact Stark widths are fitted with temperature using a logarithmic formula. Our investigation of the importance of the electron impact broadening under the physical conditions of hot DA white dwarf atmospheres shows that this mechanism is dominant nearly for all studied models, especially for the models with high surface gravity and high effective temperature. Our results may be useful for modelling white dwarf atmospheres and determining the abundance of nickel in these kinds of atmospheres. Our Stark broadening data may also be useful for research devoted to studying a possible variation of fundamental constants with gravitational potential.

No Stark broadening data have been previously determined for Ni V spectral lines, neither theoretically nor experimentally, so our results come to fill this lack. New theoretical or experimental Stark broadening parameters of Ni V spectral lines are recommended to compare our data and to check their accuracy.

ACKNOWLEDGEMENTS

The authors would like to thank the Deanship of Scientific Research at Umm Al-Qura University for supporting this work by grant code (23UQU4331237DSR04). This work has been supported by the Tunisian Laboratory of Molecular Spectroscopy and Dynamics LR18ES02 and the French Research Unit UMR8112, and by the Paris Observatory and the CNRS. We also acknowledge financial support from the Programme National de Physique Stellaire (PNPS) of CNRS/INSU, CEA, and CNES, France.

DATA AVAILABILITY

The data underlying this article are available in the article and in its online supplementary material.

REFERENCES

Al-Towyan A., Nessib N. B., Alonizan N., Qindeel R., Yacoub N., 2016, Eur. Phys. J. Plus, 131, 9
Aloui R., Elabidi H., Sahal-Bréchot S., Dimitrijević M. S., 2018, Atoms, 6, 20
Atomic spectral line database from CD-ROM 23 of R.L. Kurucz, 2023, Available at: https://lweb.cfa.harvard.edu/amp/ampdata/kurucz23/sekur.html
Berengut J. C., Flambaum V. V., Ong A., Webb J. K., Barrow J. D., Barstow M. A., Preval S. P., Holberg J. B., 2013, Phys. Rev. Lett., 111, 010801
Cowan R. D., 1981, The theory of atomic structure and spectra. University of California Press, Berkeley, USA
Cowley C. R., 1971, The Observatory, 91, 139
Dimitrijević M. S., Christova M. D., Yubero C., Sahal-Bréchot S., 2023, MNRAS, 518, 2671
Dimitrijević M. S., Konjević N., 1980, J. Quant. Spec. Radiat. Transf., 24, 451
Dimitrijević M. S., Sahal-Bréchot S., 1984, J. Quant. Spec. Radiat. Transf., 31, 301
Dimitrijević M. S., Sahal-Bréchot S., 1994, Phys. Scr, 49, 661
Dimitrijević M. S., Sahal-Bréchot S., 1996, Phys. Scr., 54, 50
Dimitrijević M. S., Sahal-Bréchot S., Bommier V., 1991, A&AS, 89, 581
Eissner W., Jones M., Nussbaumer H., 1974, Comput. Phys. Commun., 8, 270
Elabidi H., 2021, MNRAS, 503, 5730
Elabidi H., Ben Nessib N., Sahal-Bréchot S., 2004, J. Phys. B: At. Mol. Phys., 37, 63
Fleurier C., Sahal-Bréchot S., Chapelle J., 1977, JQSRT, 17, 595
Hamdi R., Ben Nessib N., Dimitrijević M. S., Sahal-Bréchot S., 2013, MNRAS, 431, 1039
Hamdi R., Ben Nessib N., Sahal Bréchot S., Dimitrijević M. S., 2017, Atoms, 5, 26
Hamdi R., Ben Nessib N., Sahal-Bréchot S., Dimitrijević M. S., 2014, Adv. Space Res., 54, 1223
Hamdi R., Ben Nessib N., Sahal-Bréchot S., Dimitrijević M. S., 2018, MNRAS, 475, 800
Hamdi R., Ben Nessib N., Sahal-Bréchot S., Dimitrijević M. S., 2019, MNRAS, 488, 2473
Hamdi R., Ben Nessib N., Sahal-Bréchot S., Dimitrijević M. S., 2021, MNRAS, 504, 1320
Hamdi R., Ben Nessib N., Sahal-Bréchot S., Dimitrijević M. S., 2022, Astron. Nachr., 343, e210047
Hu J. et al., 2021, MNRAS, 500, 1466
Konjević N., 1999, Phys. Rep., 316, 339
Le T. D., 2021, Chin. J. Phys., 73, 147
Mahmoudi W. F., Abu El Maati L., Alkallas F., Ben Nessib N., Sahal-Bréchot S., Dimitrijević M. S., 2023, Adv. Space Res., 71, 1281
Majlinger Z., Dimitrijević M. S., Srećković V. A., 2020, MNRAS, 496, 5584
Majlinger Z., Simić Z., Dimitrijević M. S., 2017, MNRAS, 470, 1911
Preval S. P. et al., 2019, MNRAS, 487, 3470
Preval S. P., Barstow M. A., Holberg J. B., Dickinson N. J., 2013, MNRAS, 436, 659
Rauch T., Gamrath S., Quinet P., Demleitner M., Knörzer M., Werner K., Kruk J. W., 2020, A&A, 637, A4
Sahal-Bréchot S., 1969a, A&A, 1, 91
Sahal-Bréchot S., 1969b, A&A, 2, 322
Sahal-Bréchot S., 1974, A&A, 35, 319
Sahal-Bréchot S., 2021, Atoms, 9, 29
Sahal-Bréchot S., Dimitrijević M. S., Ben Nessib N., 2011, Balt. Astron., 20, 523
Sahal-Bréchot S., Dimitrijević M. S., Moreau N., Ben Nessib N., 2015, Phys. Scr., 90, 054008
Sahal-Bréchot S., Dimitrijević M. S., Nessib N., 2014, Atoms, 2, 225
Sahal-Bréchot S., Elabidi H., 2021, A&A, 652, A47
Wesemael F., Auer L. H., van Horn H. M., Savedoff M. P., 1980, ApJS, 43, 159

SUPPORTING INFORMATION

Supplementary data are available at *MNRAS* online.

suppl_data

Please note: Oxford University Press is not responsible for the content or functionality of any supporting materials supplied by the authors. Any queries (other than missing material) should be directed to the corresponding author for the article.

This paper has been typeset from a TEX/LATEX file prepared by the author.